

# Amyloid- $\beta$ protein dimers isolated directly from Alzheimer's brains impair synaptic plasticity and memory

Ganesh M Shankar<sup>1,2</sup>, Shaomin Li<sup>1</sup>, Tapan H Mehta<sup>1</sup>, Amaya Garcia-Munoz<sup>3</sup>, Nina E Shepardson<sup>1</sup>, Imelda Smith<sup>4</sup>, Francesca M Brett<sup>5</sup>, Michael A Farrell<sup>5</sup>, Michael J Rowan<sup>6</sup>, Cynthia A Lemere<sup>1</sup>, Ciaran M Regan<sup>3</sup>, Dominic M Walsh<sup>4</sup>, Bernardo L Sabatini<sup>2</sup> & Dennis J Selkoe<sup>1</sup>

**Alzheimer's disease constitutes a rising threat to public health. Despite extensive research in cellular and animal models, identifying the pathogenic agent present in the human brain and showing that it confers key features of Alzheimer's disease has not been achieved. We extracted soluble amyloid- $\beta$  protein (A $\beta$ ) oligomers directly from the cerebral cortex of subjects with Alzheimer's disease. The oligomers potently inhibited long-term potentiation (LTP), enhanced long-term depression (LTD) and reduced dendritic spine density in normal rodent hippocampus. Soluble A $\beta$  from Alzheimer's disease brain also disrupted the memory of a learned behavior in normal rats. These various effects were specifically attributable to A $\beta$  dimers. Mechanistically, metabotropic glutamate receptors were required for the LTD enhancement, and *N*-methyl *D*-aspartate receptors were required for the spine loss. Co-administering antibodies to the A $\beta$  N-terminus prevented the LTP and LTD deficits, whereas antibodies to the midregion or C-terminus were less effective. Insoluble amyloid plaque cores from Alzheimer's disease cortex did not impair LTP unless they were first solubilized to release A $\beta$  dimers, suggesting that plaque cores are largely inactive but sequester A $\beta$  dimers that are synaptotoxic. We conclude that soluble A $\beta$  oligomers extracted from Alzheimer's disease brains potently impair synapse structure and function and that dimers are the smallest synaptotoxic species.**

Alzheimer's disease is distinguished histopathologically from other dementias by abundant extraneuronal deposits of A $\beta$ . Numerous reports describe neuronal alterations induced by supraphysiological concentrations of synthetic A $\beta$  peptides, by A $\beta$  species secreted by cultured cells, or by complex mixtures of A $\beta$  assembly forms in the brains of amyloid precursor protein (APP) transgenic mice<sup>1–5</sup>. Although these findings show that A $\beta$  can alter synapse physiology in experimental models, the nature of the pathogenic species in the human brain and direct demonstration of its neurobiological effects are unresolved.

To extract and characterize A $\beta$  present in human brain, we prepared aqueously soluble (Tris-buffered saline (TBS)), detergent-soluble (TBS with 1% Triton X-100) and 'insoluble' (5 M GuHCl) extracts by sequential centrifugation of brain homogenates from humans with various neuropathologically confirmed dementias (Supplementary Table 1a online). Immunoprecipitation and western blotting<sup>5,6</sup> revealed A $\beta$  monomers and lithium dodecylsulfate (LDS)-stable dimers and trimers in all three extracts of the frontal and temporal cortices from subjects with Alzheimer's disease and an adult with Down's syndrome and Alzheimer's disease (Fig. 1). Cortical extracts from some subjects without Alzheimer's disease showed modest levels of A $\beta$  in the insoluble (GuHCl) extracts (Fig. 1c) but little or none in the soluble (TBS) extracts (Fig. 1a) compared to the Alzheimer's disease cases. Notably, a subject with Alzheimer's disease histopathology but no clinical Alzheimer's disease (pathological Alzheimer's disease, P-AD) showed A $\beta$  in the insoluble but not the soluble fraction (Fig. 1). Although A $\beta$  was detectable in all three sequential extracts, we chose to characterize the physiologic effects of the TBS-soluble fraction because Alzheimer's disease dementia correlates strongly with soluble A $\beta$  abundance<sup>7–9</sup>. Indeed, the profile of our extracts suggested that levels of TBS-soluble A $\beta$  correlated best with the clinical Alzheimer's disease state (Fig. 1a,c). Moreover, we wished to focus on the earliest A $\beta$  assemblies: soluble oligomers that form initially from monomers.

We first asked whether soluble A $\beta$  from Alzheimer's disease cortex (Fig. 2a and Supplementary Table 1b) alters LTP in mouse hippocampus. TBS extracts from control (Con TBS) or Alzheimer's disease (AD TBS) cortex did not alter basal synaptic transmission or paired-pulse ratio (Supplementary Fig. 1a,b online), indicating that neurotransmitter release probability was unaffected<sup>10</sup>. Slices exposed to TBS vehicle (Veh) or Con TBS for 20 min showed robust LTP induction after high-frequency stimulation (HFS) ( $152.9 \pm 9.1\%$  and  $144.2 \pm 7.1\%$  of baseline standard field excitatory postsynaptic potentials (fEPSP) slope, respectively; Fig. 2b). In contrast, AD TBS inhibited LTP ( $111.3 \pm 3.9\%$ ,  $P < 0.05$ ; Fig. 2b). Immunodepleting AD TBS with an antiserum to A $\beta$  (R1282) prevented the LTP inhibition

<sup>1</sup>Center for Neurologic Diseases, Brigham and Women's Hospital and Harvard Medical School, 77 Avenue Louis Pasteur, Boston, Massachusetts 02115, USA.

<sup>2</sup>Department of Neurobiology, Harvard Medical School, 220 Longwood Avenue, Boston, Massachusetts 02115, USA. <sup>3</sup>School of Biomolecular and Biomedical Science, University College Dublin, Dublin 4, Ireland. <sup>4</sup>Laboratory for Neurodegenerative Research, University College Dublin, Dublin 4, Ireland. <sup>5</sup>Department of Pathology, Beaumont Hospital and Royal College of Surgeons Ireland, Dublin 9, Ireland. <sup>6</sup>Trinity College Institute of Neuroscience and Department of Pharmacology and Therapeutics, Trinity College, Dublin 2, Ireland. Correspondence should be addressed to D.J.S. (dselkoe@rics.bwh.harvard.edu).

Received 15 October 2007; accepted 15 May 2008; published online 22 June 2008; corrected online 15 July 2008 (details online); doi:10.1038/nm1782

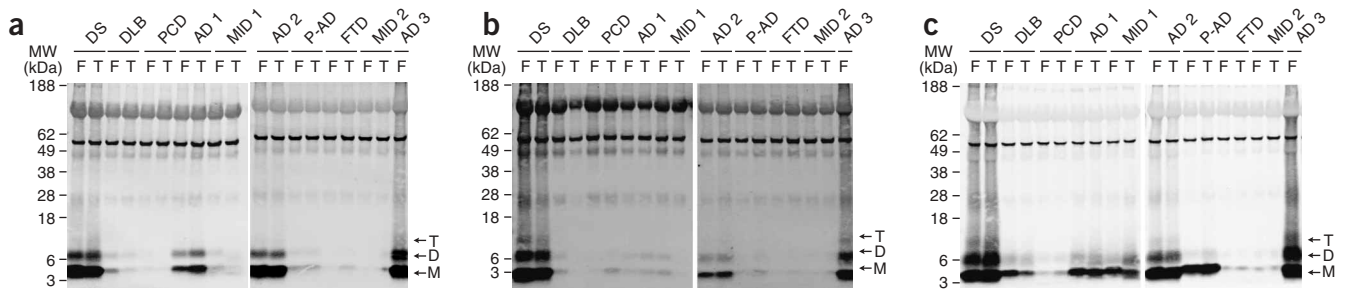


**Figure 1** Monomeric and oligomeric A $\beta$  is detected in brain extracts of humans with clinically and neuropathologically typical late-onset Alzheimer's disease. (a–c) Immunoprecipitation and western blotting (IP-WB) analysis was performed on supernatants of the soluble (a, TBS), membrane-associated (b, TBS-TX100) and insoluble (c, GuHCl) sequential extracts of frontal (F) and temporal (T) cortex homogenates from various individuals diagnosed with different forms of dementia (see **Supplementary Table 1**). Samples were immunoprecipitated with polyclonal antibody R1282 to A $\beta$  and blotted with monoclonal antibodies 2G3 (to A $\beta_{40}$ ) and 21F12 (to A $\beta_{42}$ ). DS, Down's syndrome with Alzheimer's disease; DLB, dementia with Lewy bodies; PCD, paraneoplastic cerebellar degeneration; AD, Alzheimer's disease; MMD, multi-infarct dementia; P-AD, pathological Alzheimer's disease (scattered amyloid plaques without a history of clinical Alzheimer's disease); FTD, frontotemporal dementia.

(**Fig. 2c**), indicating that A $\beta$  was necessary for the inhibition. The effect of AD TBS on LTP was strongly dose dependent (**Supplementary Fig. 1d**). Notably, TBS extracts prepared identically from the cortices of individuals with frontotemporal dementia or dementia with Lewy bodies did not significantly alter LTP ( $137.0 \pm 5.3\%$  and  $148.1 \pm 6.1\%$ , respectively) (**Fig. 2d** and **Supplementary Fig. 1e**). Additional brain extracts from two control subjects and three subjects with Alzheimer's disease fully replicated the above findings (**Fig. 2a,d**).

LTD of hippocampal synapses is induced by persistent subthreshold stimulation<sup>11</sup>. Standard protocols for LTD induction in adult rodent hippocampus require delivery of 600–900 pulses at low frequency<sup>12,13</sup>. Accordingly, 300 pulses at 1 Hz failed to induce LTD in the presence of vehicle or Con TBS (**Fig. 2e**). However, AD TBS facilitated LTD induction by this weak stimulus ( $74.7 \pm 4.8\%$  of baseline for AD TBS versus  $101.9 \pm 5.6\%$  for Con TBS,  $P < 0.05$ ; **Fig. 2e**). LTD induced with AD TBS was N-methyl-D-aspartate receptor (NMDAR) independent, as the NMDAR antagonist AP-5 did not block this effect ( $68.1 \pm 4.3\%$ ; **Fig. 2f**). However, both  $\alpha$ -methyl-4-carboxyphenylglycine (MCPG), a group I/II metabotropic glutamate receptor (mGluR) antagonist ( $94.8 \pm 2.4\%$ ,  $P < 0.05$ ), and SIB1757, an mGluR5 antagonist ( $101.1 \pm 6.9\%$ ,  $P < 0.05$ ), prevented LTD facilitation by AD TBS (**Fig. 2f**). Whereas mGluR activation was necessary for the LTD facilitation by soluble A $\beta$ , SIB1757 did not prevent AD TBS-mediated LTP inhibition (**Supplementary Fig. 1f**). This finding is consistent with earlier data showing that A $\beta$  can influence synaptic plasticity through various receptors, including NMDAR, mGluR and nicotinic acetylcholine receptors<sup>14–17</sup>.

Passive administration of monoclonal A $\beta$  antibodies has entered human testing for treatment of Alzheimer's disease. We found that the ability of a co-administered A $\beta$  antibody to block the above-mentioned LTD facilitation correlated with its ability to immunoprecipitate soluble A $\beta$  from AD TBS (**Supplementary Fig. 2** online). Antibodies to the free N-terminus of A $\beta$  (3D6; 82E1) almost completely precipitated soluble A $\beta$  from AD TBS and also prevented the LTD facilitation ( $98.4 \pm 3.0\%$ ), whereas antibodies to the A $\beta$  C-terminus (2G3, 21F12) weakly precipitated A $\beta$  and did not block the LTD effect ( $72.1 \pm 4.9\%$ ; **Supplementary Fig. 2a,b**). A $\beta$  midregion antibodies immunoprecipitated a fraction of the A $\beta$  species in AD TBS and only partially blocked the LTD effect (**Supplementary Fig. 2a,c**). Similarly, N-terminal but not C-terminal antibodies neutralized the LTP deficit (**Supplementary Fig. 2d**).

To assess the effects of soluble Alzheimer's disease cortical extracts directly on memory function, we trained rats on a step-through passive avoidance task<sup>18</sup>. At 0, 3 or 6 h after training, we injected AD TBS or R1282-immunodepleted AD TBS (AD TBS-ID) (**Supplementary Fig. 3a** online) into the lateral ventricle. AD TBS administered 3 h after training significantly impaired the rats' recall of the learned behavior 48 h later, such that the latency to enter the dark chamber, where the rat had received a shock during training, was significantly ( $P < 0.05$ ) shorter for rats injected with AD TBS than with AD TBS-ID (**Fig. 2g**). Notably, AD TBS injected at 0 or 6 h after training did not significantly alter the escape latency (**Supplementary Fig. 3**). The 3-h post-training time point at which AD TBS significantly impaired recall is consistent with the temporal pattern of transcriptional regulation of synapse remodeling following passive avoidance training<sup>19</sup>.

Decreased synapse density is the strongest neuropathological correlate of the degree of dementia in Alzheimer's disease<sup>20</sup>. To determine whether soluble A $\beta$  in Alzheimer's disease brain contributes directly to synapse loss, we quantified dendritic spine density in GFP-transfected pyramidal cells in organotypic rat hippocampal slices<sup>21</sup>. To properly reconstitute brain extracts in slice culture medium, we subjected TBS extracts to non-denaturing size-exclusion chromatography (SEC). Pyramidal neurons in slices cultured for 10 d with plain medium (sham) or medium reconstituted with lyophilized SEC fractions of Con TBS (Con TBS-SEC) showed similar spine densities ( $0.79 \pm 0.02$  and  $0.86 \pm 0.03$  spines/ $\mu\text{m}$ ,  $n = 6/890$  and  $5/628$  cells/spines, respectively). In contrast, slice medium reconstituted with SEC fractions from AD TBS (AD TBS-SEC) caused a 47% decrease in spine density versus Con TBS-SEC ( $0.46 \pm 0.03$  spines/ $\mu\text{m}$ ,  $P < 0.05$ ;  $n = 6/517$ ; **Fig. 2h** and **Supplementary Fig. 4** online). MCPG did not prevent the loss of spines with AD TBS-SEC treatment ( $0.45 \pm 0.03$  spines/ $\mu\text{m}$ ;  $n = 5/337$ ; **Fig. 2h**). 3-((R)-2-carboxypiperazin-4-yl)-propyl-1-phosphonic acid (CPP), an NMDAR antagonist, did not alter spine density when applied alone but prevented the decrease observed with AD TBS-SEC ( $0.73 \pm 0.03$  and  $0.84 \pm 0.03$ , respectively;  $n = 5/619$  and  $5/748$ ;  $P < 0.05$  for AD TBS-SEC alone versus AD TBS-SEC with CPP; **Fig. 2h**). These findings support previous evidence that NMDAR activation is necessary for A $\beta$ -mediated spine loss<sup>16,17</sup>.

We next asked which soluble A $\beta$  species present in Alzheimer's disease brain mediated these effects on synapse physiology. Two lines of evidence indicated that the A $\beta$ -immunoreactive species migrating

at 8 kDa on LDS-PAGE gels were true A $\beta$  dimers. First, mass spectrometry of the 4- and 8-kDa bands immunoprecipitated from the GuHCl extract of Alzheimer's disease cortex confirmed that each contained tryptic peptides of human A $\beta$  (Supplementary Fig. 5b–e online). Second, immunoprecipitation of this extract with an A $\beta$ <sub>40</sub>-specific antibody (2G3) and western blot analysis with an A $\beta$ <sub>42</sub>-specific antibody (21F12) revealed a heterodimer composed of A $\beta$ <sub>40</sub> and A $\beta$ <sub>42</sub> migrating at 8 kDa (Supplementary Fig. 5a). Performing this coimmunoprecipitation with 21F12 for both the immunoprecipitation and the western blot yielded a much stronger dimer signal, indicating that most of the 8-kDa species are A $\beta$ <sub>40</sub>–A $\beta$ <sub>42</sub> homodimers (Supplementary Fig. 5a).

Having confirmed that the 8-kDa bands detected by western blotting in Alzheimer's disease brain samples (Figs. 1 and 2a) are *bona fide* A $\beta$  dimers, we used nondenaturing SEC to separate the various A $\beta$  species in AD TBS and characterized their respective effects on LTP. Most of the A $\beta$  in AD TBS eluted in the void volume (fractions 3–4, >60 kDa based on co-eluting linear polydextran standards<sup>22</sup>), but this higher molecular weight complex dissociated into A $\beta$  monomers and dimers when denatured by LDS-PAGE (Fig. 3a). This SEC profile also showed dimers eluting at ~8–16 kDa (fractions 7–8) and monomers eluting at ~3–6 kDa (fractions 10–11). Taken together, these results indicate that in Alzheimer's disease cortex, soluble A $\beta$  exists in various assemblies, with the smallest native oligomer being a dimer.

To establish which soluble A $\beta$  species were responsible for the impaired synaptic plasticity, SEC fractions of AD TBS containing

either higher molecular weight complexes (AD SEC 4), native A $\beta$  dimers (AD SEC 8) or monomers (AD SEC 10) were each tested separately. Only AD SEC 8 significantly inhibited LTP ( $107.0 \pm 2.2\%$ ;  $P < 0.05$  versus Con TBS), whereas AD SEC 4, AD SEC 10 and identically prepared fractions from Con TBS were all inactive (Fig. 3b). Notably, the AD SEC 4 fraction contained the highest concentration of A $\beta$  (Fig. 3a), suggesting that the specific activity of this higher molecular weight A $\beta$  assembly is very low. To achieve a purer preparation of A $\beta$  dimers, AD TBS was immunoprecipitated with 3D6, eluted with denaturing LDS buffer and subjected to SEC (IP-SEC; Fig. 3c). Most of the soluble A $\beta$  now eluted at the size of dimers (fractions 7–8) rather than in the void volume (Supplementary Fig. 6 online), suggesting that elution with LDS disrupts noncovalent interactions among the higher molecular weight A $\beta$  assemblies. LTP was significantly inhibited by IP-SEC fractions 7–8, containing A $\beta$  dimers ( $106.6 \pm 2.4\%$ ,  $P < 0.05$ ), but not by fractions 10–11 containing monomers nor by any IP-SEC fractions from Con TBS (Fig. 3d).

Although these SEC experiments showed that soluble A $\beta$  dimers inhibit LTP, it remained possible that a small molecule from human brain was bound to the A $\beta$  dimers and was required to impair LTP. To address this possibility, we generated a synthetic A $\beta$ <sub>40</sub> peptide in which Ser26 was mutated to cysteine (A $\beta$ <sub>40</sub>-S26C). An A $\beta$  dimer was observed upon oxidation (Fig. 3e), and this inhibited LTP nearly 20 times more potently than did wild-type synthetic A $\beta$ <sub>40</sub> (Fig. 3f). This pure, synthetic dimer cannot contain any other factors present in AD TBS, establishing that A $\beta$  dimers alone are sufficient to perturb synapse physiology.

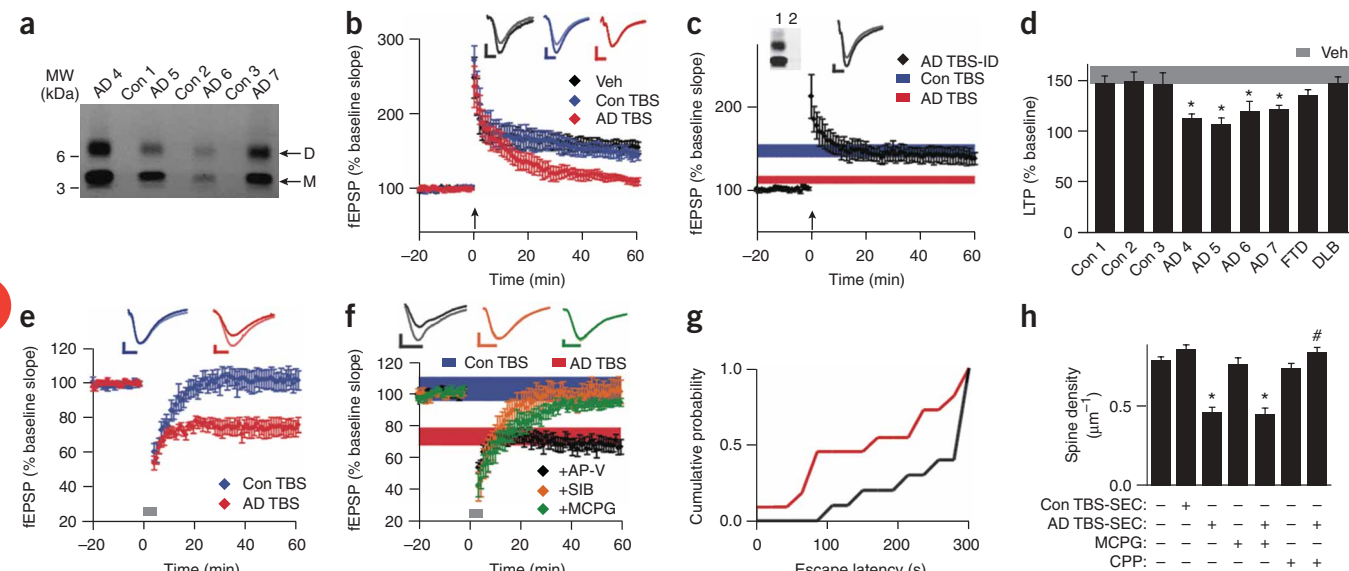
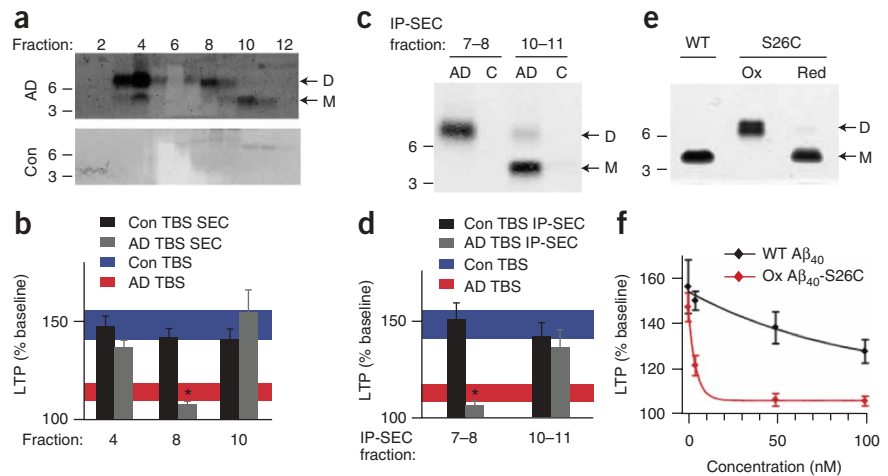


**Figure 3** Soluble dimers are the smallest A $\beta$  assembly form in human brain to acutely perturb synapse physiology. **(a)** AD TBS (top) and Con TBS (bottom) were subjected to nondenaturing SEC and blotted with 2G3 and 21F12. A $\beta$  monomer (M) and dimer (D) in AD TBS is recovered in the void volume (fractions 3 and 4). The white areas at the bottom of lanes 5–7 are intrinsic to these gels and represent an unknown soluble factor that we commonly observe in western blots of SEC fractions of human brain TBS extracts and that interferes with blocking, antibody labeling or both. **(b)** Summary LTP data (means  $\pm$  s.e.m.) for slices treated with SEC fractions characterized in **a** ( $n = 6$  slices for all samples). **(c)** IP-SEC fractionation of AD TBS generates dimer-enriched (fractions 7–8) and monomer-enriched (fractions 10–11) fractions. **(d)** Summary LTP data (means  $\pm$  s.e.m.) for slices treated with IP-SEC fractions of AD and Con TBS brain extracts, as characterized in **c** (Con TBS fractions 10–11,  $n = 5$ ; AD TBS fractions 10–11,  $n = 5$ ; Con TBS fractions 7–8,  $n = 7$ ; AD TBS fractions 7–8,  $n = 7$ ). **(e)** Silver stain showing that mutant A $\beta_{40}$ -S26C forms dimers when oxidized (ox) and can be reduced (red) to monomers with  $\beta$ -mercaptoethanol treatment. **(f)** Summary LTP data (means  $\pm$  s.e.m.) for slices treated with either WT A $\beta_{40}$  (black) or oxidized A $\beta_{40}$ -S26C (red) reveals that the oxidized A $\beta_{40}$ -S26C dimer inhibits LTP with much greater potency (100 nM A $\beta_{40}$ -S26C,  $n = 4$ ;  $n = 5$  for all other treatments). The vehicle controls (plotted at 0 nM) were 50 mM ammonium acetate ( $n = 4$ ) for the S26C peptide and 0.1% ammonium hydroxide ( $n = 4$ ) for the WT peptide.



Previous studies have suggested that unlike soluble A $\beta$  abundance, amyloid plaque burden correlates poorly with Alzheimer's disease severity<sup>7,9,20</sup>. We asked whether insoluble amyloid cores isolated from Alzheimer's disease cortex can inhibit hippocampal LTP. To isolate these detergent-resistant foci of fibrillar A $\beta$  from neuritic plaques<sup>23–25</sup>, we homogenized TBS-insoluble pellets of plaque-rich Alzheimer's disease cortex in 2% SDS<sup>24</sup>. Immunoprecipitation and western blotting of supernatants after washing in SDS buffer showed that no additional A $\beta$  was liberated by SDS or TBS from this preparation (Fig. 4a). Congo red staining of the residual pellet revealed intact amyloid cores showing characteristic birefringence (Fig. 4b). Although resistant to disruption by many solvents, Alzheimer's disease amyloid cores are efficiently solubilized by formic acid<sup>23,24</sup>. This treatment released A $\beta$  dimers and monomers from the washed cores (Fig. 4a). When we applied this formic acid extract of

the Alzheimer's disease core preparation to hippocampal slices, LTP was inhibited ( $116.2 \pm 4.6\%$ ,  $P < 0.05$  versus formic acid vehicle; Fig. 4c). Formic acid extracts of identically prepared fractions from control brain allowed normal LTP (Fig. 4c). Thus, amyloid cores contain A $\beta$  dimers that can impair synaptic plasticity. In contrast, addition of intact cores (Fig. 4b) to the artificial cerebrospinal fluid (ACSF) perfusate did not affect LTP ( $139.4 \pm 7.6\%$ , Fig. 4d). Therefore, in physiologic buffer (ACSF), amyloid cores do not acutely release soluble A $\beta$  dimers to alter synaptic plasticity. Immunoprecipitation and western blot analysis revealed that A $\beta$  dimers also were not released from amyloid cores incubated in physiological buffers at 37 °C for 24 h (Supplementary Fig. 7 online), suggesting that highly insoluble A $\beta$  aggregates such as amyloid plaque cores represent dimer-rich structures that do not readily dissociate.

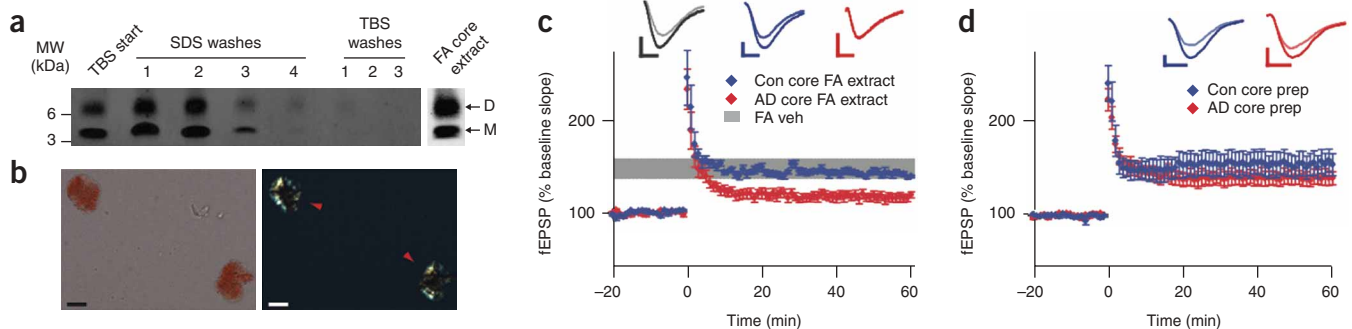


**Figure 4** Insoluble amyloid cores contain A $\beta$  dimers with synaptotoxic potential but are not readily released. **(a)** IP-WB of sequential extracts of the TBS-insoluble pellet prepared from 100 mg of a plaque-rich Alzheimer's disease brain (case AD 5 from Fig. 2a). The final TBS washes reveal that no additional soluble A $\beta$  can be extracted from the pellet after four sequential SDS washes. The remaining core-rich pellet was then incubated in formic acid (FA core extract) and analyzed by IP-WB, revealing that the insoluble cores contain A $\beta$  monomers and dimers (far right lane). **(b)** Core preparations after the final TBS wash in **a** were stained with 0.2% Congo red and visualized by brightfield (left) and polarization (right) microscopy. Isolated amyloid cores show characteristic birefringence with Congo red (red arrowheads). Material prepared similarly from Con 3 (Fig. 2a) did not contain any such structures. Scale bar, 5  $\mu$ m. **(c)** Cores prepared as in **a** and **b** were extracted with 88% formic acid and neutralized with NaOH. Summary LTP data for slices treated with just FA and NaOH vehicle (FA Veh,  $n = 5$ ), or with FA and NaOH core extracts from Alzheimer's disease (AD core FA extract,  $n = 7$ ) or control (Con core FA extract,  $n = 5$ ) brains. Calibration bars, 5 msec/0.2 mV. **(d)** Summary LTP data for slices exposed to intact core preps isolated as in **a** and **b** from 100 mg Alzheimer's disease cortex (AD core prep,  $n = 5$ ) or Con cortex (Con core prep,  $n = 5$ ). Calibration bars, 5 msec/0.3 mV.

Here we show that soluble A $\beta$  isolated directly from Alzheimer's disease brains potently and consistently induces several Alzheimer's disease-like phenotypes in normal adult rodents: it decreases dendritic spine density, inhibits LTP and facilitates LTD in hippocampus, and interferes with the memory of a learned behavior. We used nondenaturing gel filtration coupled with immunoprecipitation and western blotting and subsequent immunodepletion or neutralization with epitope-specific antibodies to A $\beta$  to ascribe the pathogenic effects to soluble A $\beta$  oligomers, principally dimers.

Our findings support the emerging concept that the effects of A $\beta$  in Alzheimer's disease initially center on subtly altered synapse function. Neither A $\beta$  monomers nor insoluble amyloid plaque cores significantly altered synaptic plasticity. This does not mean that insoluble amyloid plaques have no pathogenic role; their invariant accumulation may signify that they serve as relatively inert reservoirs of small bioactive oligomers, and they may disassemble more readily in the presence of lipids<sup>26</sup>. That plaque cores may release locally active A $\beta$  species *in vivo* is suggested by a penumbra of synapse loss around cores in APP transgenic mice<sup>27</sup>.

Our examination of soluble dimers obtained from Alzheimer's disease brain is partially consistent with findings using synthetic<sup>2</sup> or cell-derived<sup>5,28</sup> A $\beta$  oligomers. However, there are unresolved differences regarding the precise biochemical nature of the synaptotoxic species found in these various systems. For example, we did not detect in human cortical extracts (Fig. 1 and Supplementary Fig. 6) a soluble, SDS-stable dodecamer of A $\beta$ , similar to the A $\beta$ \*56 species observed in brain extracts from certain APP transgenic mice<sup>29</sup>. Soluble A $\beta$  complexes from Alzheimer's disease cortex eluted in the void volume (>70 kDa) upon nondenaturing SEC, but these dissociated into dimers and monomers upon LDS-PAGE. Some Alzheimer's disease and aged control cerebrospinal fluid samples that contain soluble A $\beta$  dimers were recently shown to impair LTP<sup>30</sup>, a finding consistent with our data. However, the invariant detection of dimers in the soluble fraction of Alzheimer's disease cortex and their multiple synaptic effects strongly suggest that cortical dimers contribute directly to synapse dysfunction in people with Alzheimer's disease, whereas any additional effects of cerebrospinal fluid dimers in the minority of Alzheimer's disease subjects who have them<sup>30</sup> remain to be determined.

Mechanistically, we show that soluble A $\beta$  dimers from Alzheimer's disease cortex induce their effects by perturbing glutamatergic synaptic transmission. Although we find that mGluRs are required for the induction of LTD, whereas NMDARs are needed for spine loss, these receptors are unlikely to be the sole effector targets of soluble A $\beta$  oligomers. A $\beta$  extracted from human brain can now serve as the most pathophysiologically relevant material for further pathway analysis and for preclinical validation of agents designed to neutralize A $\beta$  aggregates. Our findings fulfill an essential requirement for establishing disease causation in Alzheimer's disease.

## METHODS

**Human brain sample preparation.** We collected brain specimens from deceased human subjects at autopsy after obtaining informed consent from the next of kin under protocols approved by the Partners Human Research Committee at Brigham and Women's Hospital and the Ethics Review Committee/Institutional Review Board at Beaumont Hospital in Dublin, Ireland. Each subject's clinical and neuropathological diagnoses are provided in Supplementary Table 1 online. We weighed frozen human temporal or frontal cortices containing white and gray matter, added freshly prepared, ice-cold TBS consisting of 20 mM Tris-HCl, 150 mM NaCl, pH 7.4 to the frozen cortex at 4:1 (TBS volume / brain wet weight) and homogenized with 25 strokes at a setting of 10 on a mechanical Dounce homogenizer. We spun the homogenate at

175,000g in a TLA100.2 rotor on a Beckman TL 100 centrifuge. We aliquoted and then stored the supernatant (called TBS extract) at  $-80^{\circ}\text{C}$ , and we rehomogenized the pellet (4:1 vol/wt) in TBS plus 1% Triton X-100 and spun as above. The resultant supernatant (called TBS-TX extract) was aliquoted and stored at  $-80^{\circ}\text{C}$ , and the pellet was rehomogenized in TBS plus 5 M guanidine HCl, pH 8.0, and incubated on a Nutator for 12–16 h at  $22^{\circ}\text{C}$ ; the resultant supernatant (GuHCl extract) was aliquoted and stored at  $-80^{\circ}\text{C}$ .

**Size exclusion chromatography.** We injected 1-ml aliquots of the TBS-soluble Alzheimer's disease brain extract onto a Superdex 75 (10/30HR) column (Amersham Biosciences) and eluted at a flow rate of 1 ml/min into 1-ml SEC fractions using 50 mM ammonium acetate, pH 8.5. We removed 750  $\mu\text{l}$  and stored it at  $-80^{\circ}\text{C}$ . We lyophilized the remaining 250  $\mu\text{l}$ , reconstituted it in 15  $\mu\text{l}$  of  $2\times$  LDS sample buffer, heated it at  $70^{\circ}\text{C}$  for 5 min and electrophoresed it on a 26-well 4–12% bis-Tris gel using MES running buffer (Invitrogen). We transferred proteins to 0.2- $\mu\text{m}$  nitrocellulose and western blotted for A $\beta$  with 1  $\mu\text{g/ml}$  2G3 and 21F12 (gifts of Elan) using the LiCor Odyssey Infrared Imaging System. We polled SEC fractions containing higher order A $\beta$  assemblies, LDS-stable A $\beta$  dimers or A $\beta$  monomers separately before lyophilizing them into 450- $\mu\text{l}$  aliquots.

**Immunoprecipitation and western blotting analysis of A $\beta$  in human brain extracts.** We used an immunoprecipitation and western blotting protocol described previously<sup>6</sup> to detect A $\beta$  in the TBS, TBS-TX and GuHCl extracts. We immunoprecipitated TBS extracts directly with either polyclonal antiserum R1282 to A $\beta$  (1:50) plus Protein A sepharose (PAS; Sigma) or monoclonal antibodies to A $\beta$  3D6 (3  $\mu\text{g/ml}$ ) or 2G3 and 21F12 (each at 3  $\mu\text{g/ml}$ ; gifts of Elan) plus Protein G agarose (PGA; Roche) and PAS. We diluted GuHCl extracts 1:40 in DMEM and then immunoprecipitated with R1282 (at 1:50) and PAS or with 2  $\mu\text{g/ml}$  266, 2G3 and 21F12 and PGA and PAS. We used the SilverQuest kit fast protocol (Invitrogen) for silver staining.

**Hippocampal slice electrophysiology recording.** The Harvard Medical School Standing Committee on Animals approved all experiments involving mice and rats used for electrophysiology and dendritic spine analysis. We recorded fEPSP in the CA1 region of the mouse hippocampus. We placed a unipolar stimulating electrode (World Precision Instruments) in the Schaffer collaterals of CA3 neurons to deliver test and conditioning stimuli. We positioned a borosilicate glass recording electrode filled with ACSF in stratum radiatum of CA1 200–300  $\mu\text{m}$  from the stimulating electrode. We induced fEPSPs in CA1 by two test stimuli at 0.05 Hz with an intensity that elicited a fEPSP amplitude  $\sim 40$ –50% of maximum. Once we had attained a stable test response for at least 30–60 min, we added experimental treatments to the 9.5-ml ACSF perfusate and recorded a baseline for an additional 20 min. These treatments included: 500  $\mu\text{l}$  TBS extract, 500  $\mu\text{l}$  TBS vehicle, 50  $\mu\text{M}$  AP-5, 500  $\mu\text{M}$  (R/S)-MCPG (Tocris) and 3  $\mu\text{M}$  SIB1757. The lyophilized 450- $\mu\text{l}$  aliquots of SEC fractions of GuHCl extracts described above were reconstituted in 500  $\mu\text{l}$  ACSF and added to the slice perfusates. To induce LTP, we applied two consecutive trains (1 s) of stimuli at 100 Hz separated by 20 s, a protocol that induced LTP lasting approximately 1.5 h in wild-type mice of this genetic background. To induce LTD, we delivered 300 pulses at 1 Hz. We amplified the field potentials  $100\times$  with an Axon Instruments 200B amplifier and digitized with Digidata 1322A. We sampled the data at 10 kHz and filtered them at 2 kHz. We obtained traces by pClamp 9.2 and analyzed them with the Clampfit 9.2 program. The LTP and LTD values reported throughout were measured at 60 min after the conditioning stimulus unless stated otherwise. We monitored paired-pulse responses at 50-ms inter-stimulus intervals. We calculated the facilitation ratio as fEPSP2 slope/fEPSP1 slope.

**Passive avoidance conditioning.** We performed passive avoidance training as described previously<sup>18</sup> (see Supplementary Methods online). We gave Wistar rats AD TBS or AD TBS immunodepleted with R1282 at 0, 3 or 6 h after training. We evaluated recall of the passive avoidance conditioning 24 and 48 h after training by recording the latency to enter the dark chamber, with a criterion time of 300 s.

**Dendritic spine density analysis.** We prepared, treated, imaged and analyzed the apical dendrites of pyramidal cells in organotypic hippocampal slices as

previously described<sup>17</sup> (see **Supplementary Methods**). We treated slices for 10 d with AD TBS-SEC or Con TBS-SEC. We performed pharmacologic treatments with 20  $\mu$ M D-CPP or 500  $\mu$ M (R/S)-MCPG in the presence or absence of AD TBS-SEC for 10 d.

**Statistical analyses.** Data from the electrophysiology and passive avoidance experiments were analyzed by one-way analysis of variance (ANOVA) followed by the Bonferroni *post-hoc* test to determine statistical significance. Dendritic spine morphology data were analyzed by one-way ANOVA with Tukey-Kramer's correction for multiple pairwise comparisons.

*Note: Supplementary information is available on the Nature Medicine website.*

#### ACKNOWLEDGMENTS

We thank Elan for the gifts of 2G3 and 21F12 antibodies. Mass spectrometry was performed by the Taplin Biological Mass Spectrometry Facility (S. Gygi). We thank X. Sun and W. Qiu for performing ELISA. We thank members of the Selkoe laboratory for helpful comments. G.M.S. recognizes L. Gurumani for support and encouragement. This work was supported by the US National Institute on Aging grant AG R01 027443 (D.J.S., G.M.S., S.L., T.H.M., N.E.S.), Science Foundation Ireland grant 03/IN3/B403C (C.M.R., A.G.-M.) and Wellcome Trust grant 067660 (D.M.W., I.S.). B.L.S. was supported by the McKnight and Ellison Foundations as well as by a Lefler Small Grant Fund.

#### AUTHOR CONTRIBUTIONS

G.M.S. designed and performed experiments and prepared the manuscript; S.L. designed and performed electrophysiology experiments; T.H.M. and N.E.S. performed biochemical experiments; A.G.-M. performed passive avoidance experiments; I.S. generated mutant A $\beta$  peptide; C.A.L., F.M.B. and M.A.F. characterized human brain tissue; M.J.R. designed electrophysiology experiments; C.M.R. designed passive avoidance experiments; D.M.W. designed biochemical experiments; B.L.S. designed electrophysiology and morphology experiments; and D.J.S. designed experiments and prepared the manuscript.

#### COMPETING INTERESTS STATEMENT

The authors declare competing financial interests: details accompany the full-text HTML version of the paper at <http://www.nature.com/naturemedicine/>.

Published online at <http://www.nature.com/naturemedicine/>

Reprints and permissions information is available online at <http://npg.nature.com/reprintsandpermissions/>

- Lorenzo, A. & Yankner, B.A.  $\beta$ -amyloid neurotoxicity requires fibril formation and is inhibited by congo red. *Proc. Natl. Acad. Sci. USA* **91**, 12243–12247 (1994).
- Lambert, M.P. *et al.* Diffusible, nonfibrillar ligands derived from A $\beta$ 1–42 are potent central nervous system neurotoxins. *Proc. Natl. Acad. Sci. USA* **95**, 6448–6453 (1998).
- Mucke, L. *et al.* High-level neuronal expression of A $\beta$  1–42 in wild-type human amyloid protein precursor transgenic mice: synaptotoxicity without plaque formation. *J. Neurosci.* **20**, 4050–4058 (2000).
- Morgan, D. *et al.* A $\beta$  peptide vaccination prevents memory loss in an animal model of Alzheimer's disease. *Nature* **408**, 982–985 (2000).
- Walsh, D.M. *et al.* Naturally secreted oligomers of amyloid  $\beta$  protein potently inhibit hippocampal long-term potentiation *in vivo*. *Nature* **416**, 535–539 (2002).
- Walsh, D.M., Tseng, B.P., Rydel, R.E., Podlisky, M.B. & Selkoe, D.J. The oligomerization of amyloid  $\beta$  protein begins intracellularly in cells derived from human brain. *Biochemistry* **39**, 10831–10839 (2000).
- McLean, C.A. *et al.* Soluble pool of A $\beta$  amyloid as a determinant of severity of neurodegeneration in Alzheimer's disease. *Ann. Neurol.* **46**, 860–866 (1999).
- Kuo, Y.M. *et al.* Water-soluble A $\beta$  (N-40, N-42) oligomers in normal and Alzheimer disease brains. *J. Biol. Chem.* **271**, 4077–4081 (1996).
- Lue, L.F. *et al.* Soluble amyloid  $\beta$  peptide concentration as a predictor of synaptic change in Alzheimer's disease. *Am. J. Pathol.* **155**, 853–862 (1999).
- Schulz, P.E., Cook, E.P. & Johnston, D. Changes in paired-pulse facilitation suggest presynaptic involvement in long-term potentiation. *J. Neurosci.* **14**, 5325–5337 (1994).
- Kemp, N. & Bashir, Z.I. Long-term depression: a cascade of induction and expression mechanisms. *Prog. Neurobiol.* **65**, 339–365 (2001).
- Dudek, S.M. & Bear, M.F. Homosynaptic long-term depression in area CA1 of hippocampus and effects of N-methyl-D-aspartate receptor blockade. *Proc. Natl. Acad. Sci. USA* **89**, 4363–4367 (1992).
- Mulkey, R.M. & Malenka, R.C. Mechanisms underlying induction of homosynaptic long-term depression in area CA1 of the hippocampus. *Neuron* **9**, 967–975 (1992).
- Tyszkiewicz, J.P. & Yan, Z.  $\beta$ -Amyloid peptides impair PKC-dependent functions of metabotropic glutamate receptors in prefrontal cortical neurons. *J. Neurophysiol.* **93**, 3102–3111 (2005).
- Hsieh, H. *et al.* AMPAR removal underlies A $\beta$ -induced synaptic depression and dendritic spine loss. *Neuron* **52**, 831–843 (2006).
- Lacor, P.N. *et al.* A $\beta$  oligomer-induced aberrations in synapse composition, shape, and density provide a molecular basis for loss of connectivity in Alzheimer's disease. *J. Neurosci.* **27**, 796–807 (2007).
- Shankar, G.M. *et al.* Natural oligomers of the Alzheimer amyloid- $\beta$  protein induce reversible synapse loss by modulating an NMDA-type glutamate receptor-dependent signaling pathway. *J. Neurosci.* **27**, 2866–2875 (2007).
- Fox, G.B., O'Connell, A.W., Murphy, K.J. & Regan, C.M. Memory consolidation induces a transient and time-dependent increase in the frequency of neural cell adhesion molecule polysialylated cells in the adult rat hippocampus. *J. Neurochem.* **65**, 2796–2799 (1995).
- O'Sullivan, N.C. *et al.* Temporal change in gene expression in the rat dentate gyrus following passive avoidance learning. *J. Neurochem.* **101**, 1085–1098 (2007).
- Terry, R.D. *et al.* Physical basis of cognitive alterations in Alzheimer's disease: synapse loss is the major correlate of cognitive impairment. *Ann. Neurol.* **30**, 572–580 (1991).
- Tavazoie, S.F., Alvarez, V.A., Ridenour, D.A., Kwiatkowski, D.J. & Sabatini, B.L. Regulation of neuronal morphology and function by the tumor suppressors Tsc1 and Tsc2. *Nat. Neurosci.* **8**, 1727–1734 (2005).
- Walsh, D.M. *et al.* Certain inhibitors of synthetic amyloid  $\beta$ -peptide (A $\beta$ ) fibrillogenesis block oligomerization of natural A $\beta$  and thereby rescue long-term potentiation. *J. Neurosci.* **25**, 2455–2462 (2005).
- Masters, C.L. *et al.* Amyloid plaque core protein in Alzheimer disease and Down syndrome. *Proc. Natl. Acad. Sci. USA* **82**, 4245–4249 (1985).
- Selkoe, D.J., Abraham, C.R., Podlisky, M.B. & Duffy, L.K. Isolation of low-molecular-weight proteins from amyloid plaque fibers in Alzheimer's disease. *J. Neurochem.* **46**, 1820–1834 (1986).
- Roher, A.E., Palmer, K.C., Yurewicz, E.C., Ball, M.J. & Greenberg, B.D. Morphological and biochemical analyses of amyloid plaque core proteins purified from Alzheimer disease brain tissue. *J. Neurochem.* **61**, 1916–1926 (1993).
- Martins, I.C. *et al.* Lipids revert inert A $\beta$  amyloid fibrils to neurotoxic protofibrils that affect learning in mice. *EMBO J.* **27**, 224–233 (2008).
- Spires, T.L. *et al.* Dendritic spine abnormalities in amyloid precursor protein transgenic mice demonstrated by gene transfer and intravitral multiphoton microscopy. *J. Neurosci.* **25**, 7278–7287 (2005).
- Cleary, J.P. *et al.* Natural oligomers of the amyloid- $\beta$  protein specifically disrupt cognitive function. *Nat. Neurosci.* **8**, 79–84 (2005).
- Lesne, S. *et al.* A specific amyloid- $\beta$  protein assembly in the brain impairs memory. *Nature* **440**, 352–357 (2006).
- Klyubin, I. *et al.* Amyloid  $\beta$  protein dimer-containing human CSF disrupts synaptic plasticity: prevention by systemic passive immunization. *J. Neurosci.* **28**, 4231–4237 (2008).

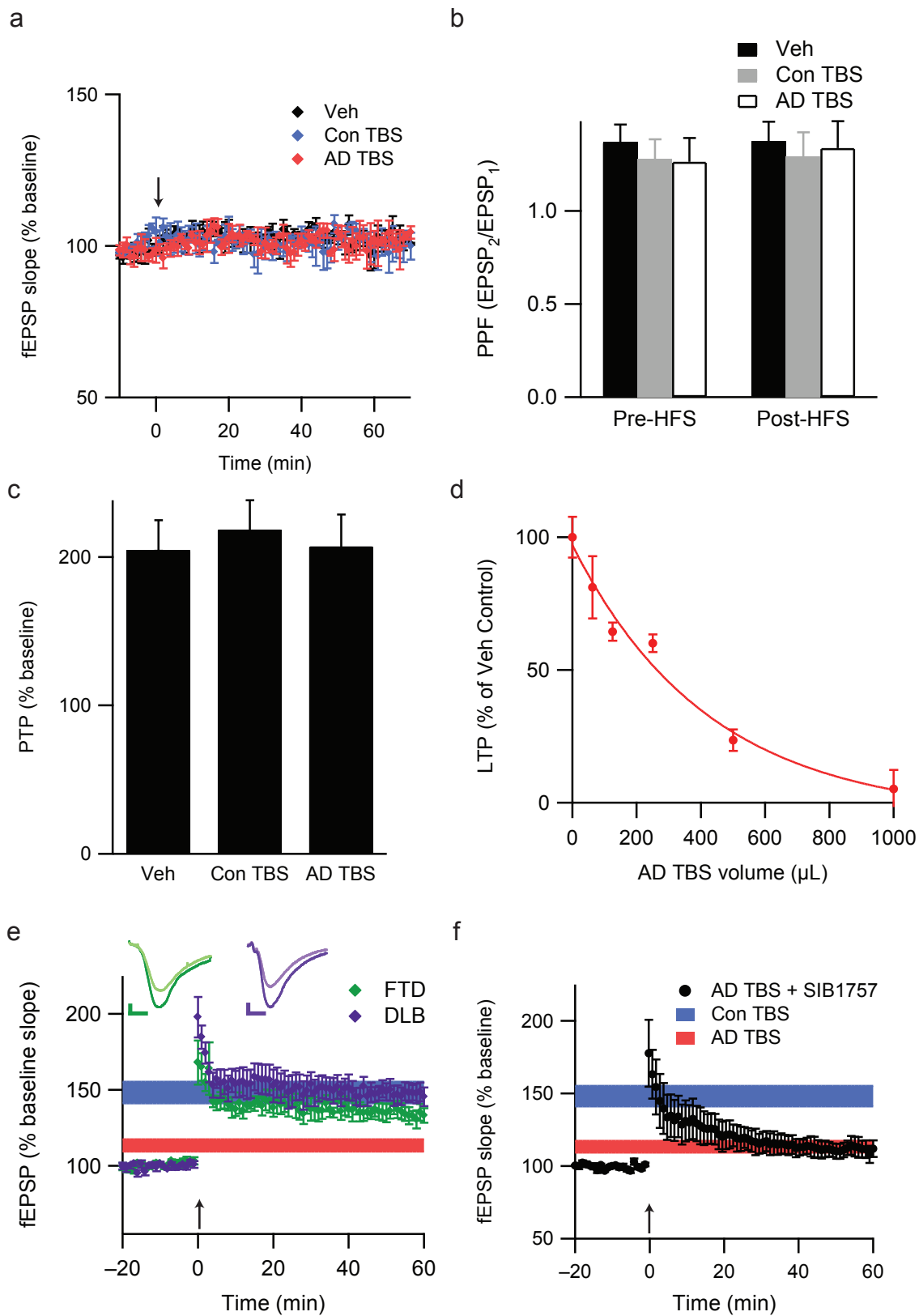
## Amyloid $\beta$ -Protein Dimers Isolated Directly from Alzheimer Brains Impair Synaptic Plasticity and Memory

Ganesh M. Shankar, Shaomin Li, Tapan H. Mehta, Amaya Garcia-Munoz, Nina E. Shepardson, Imelda Smith, Francesca M. Brett, Michael A. Farrell, Michael J. Rowan, Cynthia A. Lemere, Ciaran M. Regan, Dominic M. Walsh, Bernardo L. Sabatini and Dennis J. Selkoe

### SUPPLEMENTAL FIGURES

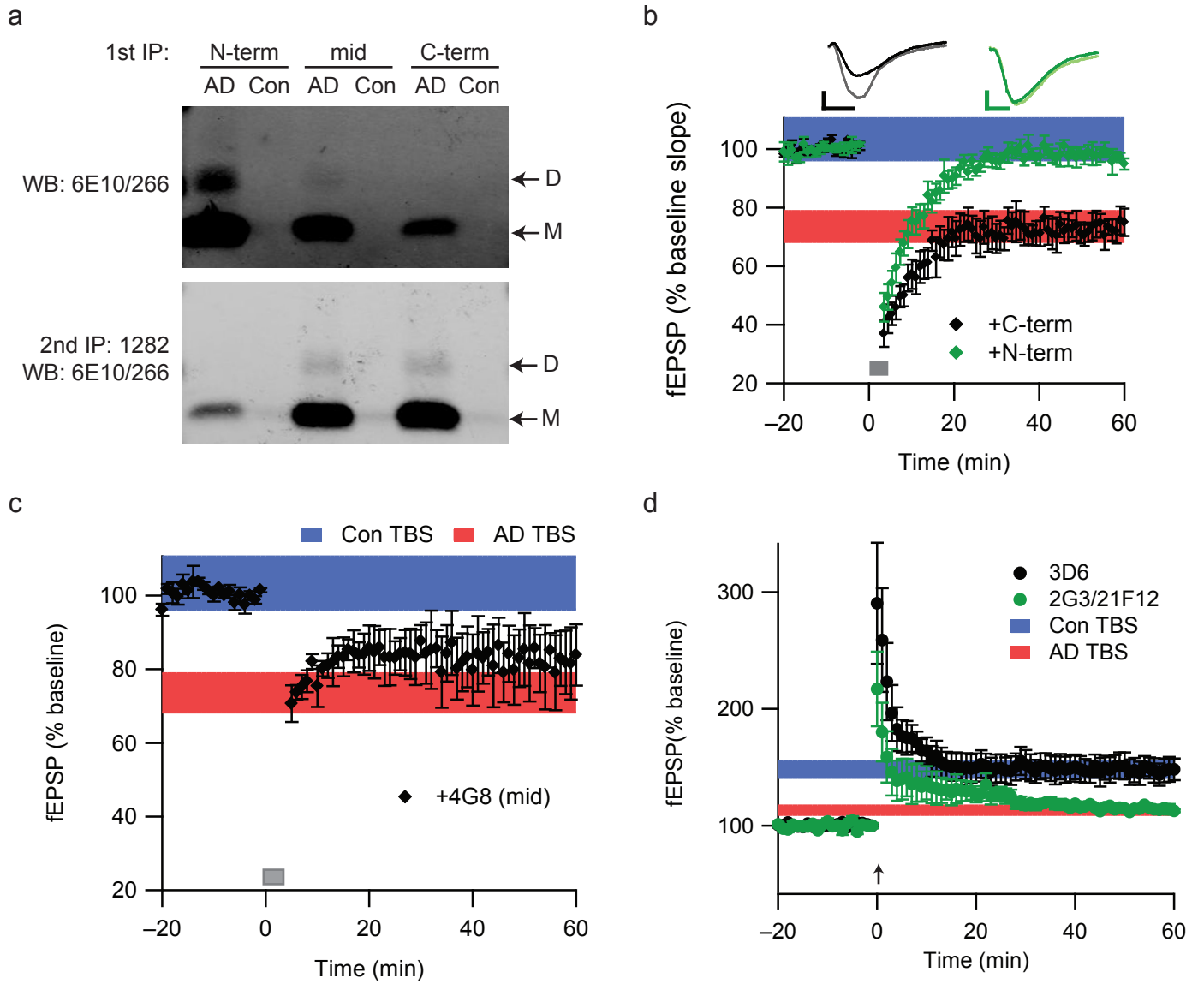
**Supplemental Figure 1.** AD soluble (TBS) brain extract does not affect baseline synaptic transmission or presynaptic release probability, but causes dose dependent LTP inhibition. **a.** After recording fEPSPs for 10 min, 500  $\mu$ L TBS Veh, Con TBS extract or AD TBS extract were added to the ACSF bath (time indicated by arrow). fEPSPs were recorded for an additional 70 min following this wash-in. **b.** Paired pulse facilitation (PPF) was calculated from the slope of the two fEPSPs resulting from an inter-stimulus interval of 50 msec. ANOVA was performed on average PPF 5 min prior to HFS (Pre-HFS) or for 55–60 min after HFS (post-HFS) from slices exposed to TBS Veh, Con TBS or AD TBS. **c.** Post-tetanic potentiation (PTP) calculated from fEPSPs recorded 5 min following HFS. **d.** The LTP inhibition by A $\beta$  in the soluble (TBS) extract of AD cortex is dose dependent. Data are plotted as percentages of optimal LTP (i.e., that obtained in 500  $\mu$ L plain TBS) measured at 50–60 min following HFS. Each dose is indicated on the abscissa as the volume of AD TBS extract that was added to a volume of plain TBS to yield a final sample volume of 500  $\mu$ L. In the case of the 500  $\mu$ L and 1000  $\mu$ L samples, the AD TBS extract was added straight. Dashed line indicates approximation of IC<sub>50</sub> value for AD TBS, which corresponds to a final A $\beta$  concentration of  $\sim$ 7 pM in the slice perfusate. **e.** TBS cortical extracts from humans with confirmed frontotemporal dementia (FTD, Fig. 1) or dementia with Lewy bodies (DLB, Fig. 1) do not inhibit LTP induction. Summary data for LTP induction in slices treated with 500  $\mu$ L TBS extracts of brains with either FTD (green) or DLB (purple). For comparison, LTP data from Fig. 2b (means  $\pm$  SEM) for Con TBS (blue) and AD TBS (red) are shown as horizontal bars. **f.** The mGluR5 antagonist SIB1757 does not block the effect of AD TBS on LTP. Summary LTP data for co-administration of 3  $\mu$ M SIB1757 with 500  $\mu$ L AD TBS (n=5 slices) for 20 minutes prior to the HFS (indicated by arrow). For comparison, LTP data from Fig. 2b (means  $\pm$  SEM) for Con TBS (blue) and AD TBS (red) are shown as horizontal bars.

Supplemental Figure 1



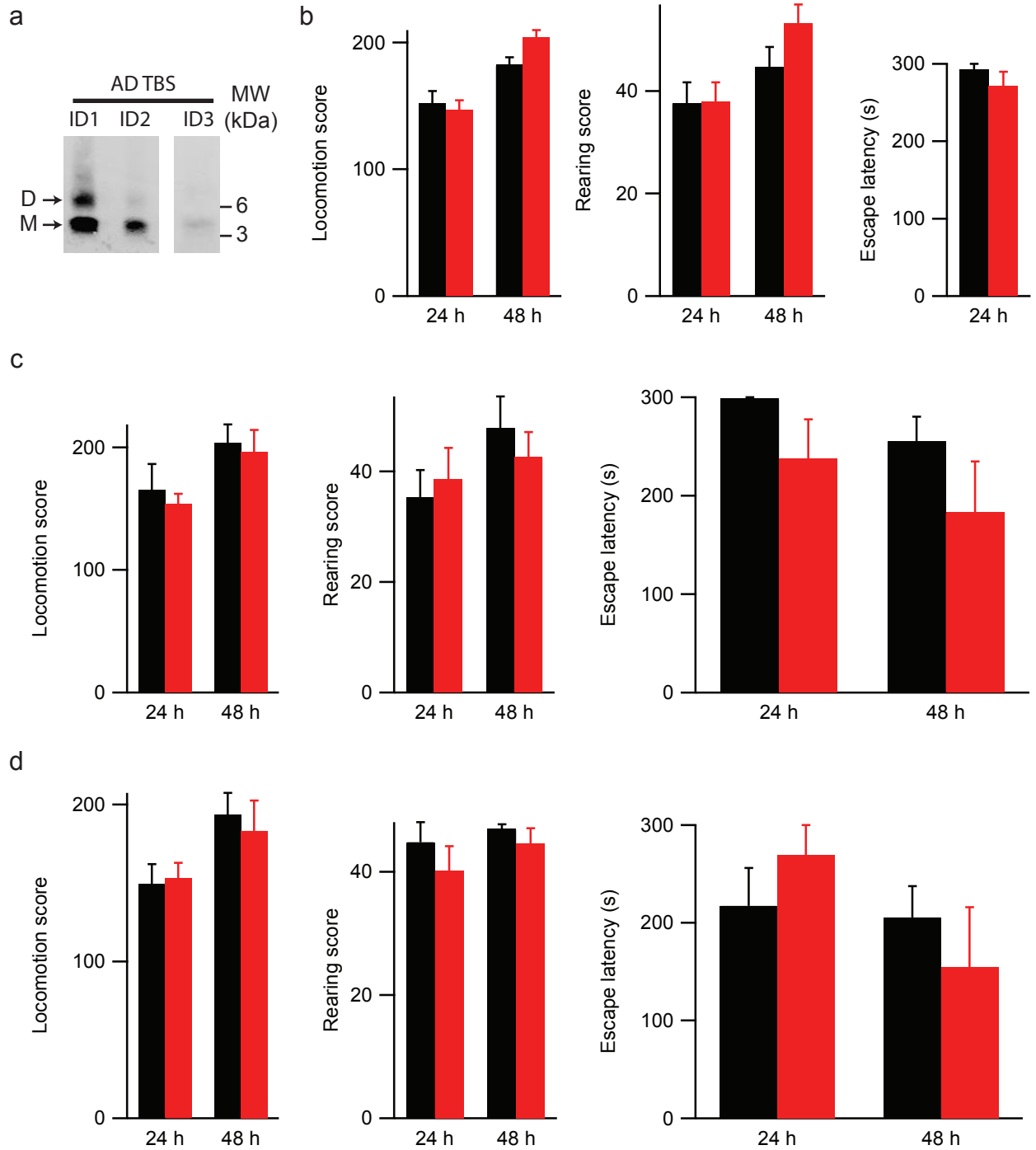
**Supplemental Figure 2.** N-terminal antibodies recognize A $\beta$  dimers and neutralize their effects on synaptic plasticity more effectively than antibodies targeting the A $\beta$  mid-region. **a.** AD TBS and Con TBS was first IP'd with 3  $\mu$ g/mL of either 3D6 (N-term), 4G8 (mid) or 2G3/21F12 (C-term) A $\beta$  antibodies (see text) and probed with A $\beta$  antibodies 6E10 plus 266. The sup after this first IP was then IP'ed with polyclonal A $\beta$  antibody R1282 (2<sup>nd</sup> IP) and probed with 6E10 plus 266 to detect remaining A $\beta$  species. **b.** Summary LTD data for co-administration of AD TBS with 3  $\mu$ g/mL of N-terminal (+N-term, green) or C-terminal (+C-term, black) A $\beta$  antibodies. LTD data (means  $\pm$  SEM) for Con TBS (blue) and AD TBS (red) are shown as horizontal bars. **c.** Summary LTD data (means  $\pm$  SEM) for co-administration of AD TBS with 3  $\mu$ g/mL 4G8 (+4G8, black, n=3 slices) for 20 min prior to LFS (grey bar). LTD data for Con TBS (blue) and AD TBS (red) from Fig. 2e are shown as horizontal bars. **d.** Summary LTP data (means  $\pm$  SEM) for co-administration of AD TBS with 3  $\mu$ g/mL 3D6 (N-term, black, n=5 slices) or 2G3/21F12 (C-term, green, n=5 slices) for 20 min prior to HFS (arrow). LTD data for Con TBS (blue) and AD TBS (red) are shown as horizontal bars.

Supplemental Figure 2



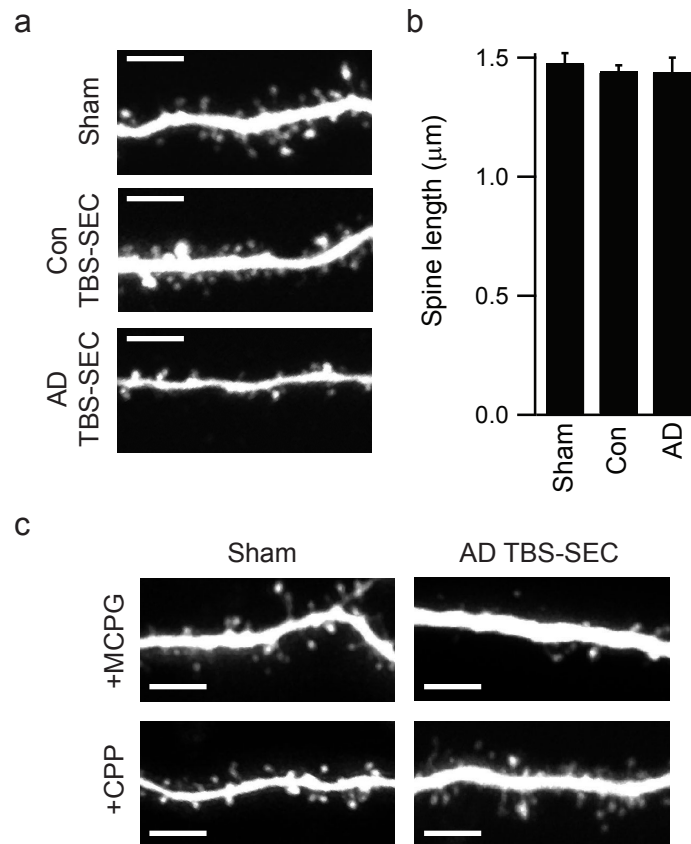
**Supplemental Figure 3.** Introduction of AD TBS at either 0 h or 6 h following training in a passive avoidance paradigm does not significantly impair the recall of this learned behavior. **a.** WB of three sequential IP's of the TBS extract (AD TBS). AD TBS-ID is the TBS supernatant remaining after the third immunodepletion (ID3). AD TBS (red) or AD TBS-ID (immunodepleted, black) was introduced i.c.v. into the lateral ventricle at either **(b)** 3 h, or **(c)** 0 h, or **(d)** 6 h following training. No significant differences between the two treatment groups were observed in locomotion scores (left) or rearing scores (middle) measured at 48 or 24 h prior to training. Furthermore, the escape latency (right) was not significantly different at 24 h or 48 h post-training when comparing rats receiving AD TBS (n=5 and 5 rats for injections at 0 h and 6 h) or AD TBS-ID (also n=5 and 5). While the escape latency was not significantly different at 24 h post-training between rats treated at 3 h with AD TBS or AD TBS-ID (b, right), a significant difference was observed at 48 h (see Fig. 2g).

# Supplemental Figure 3



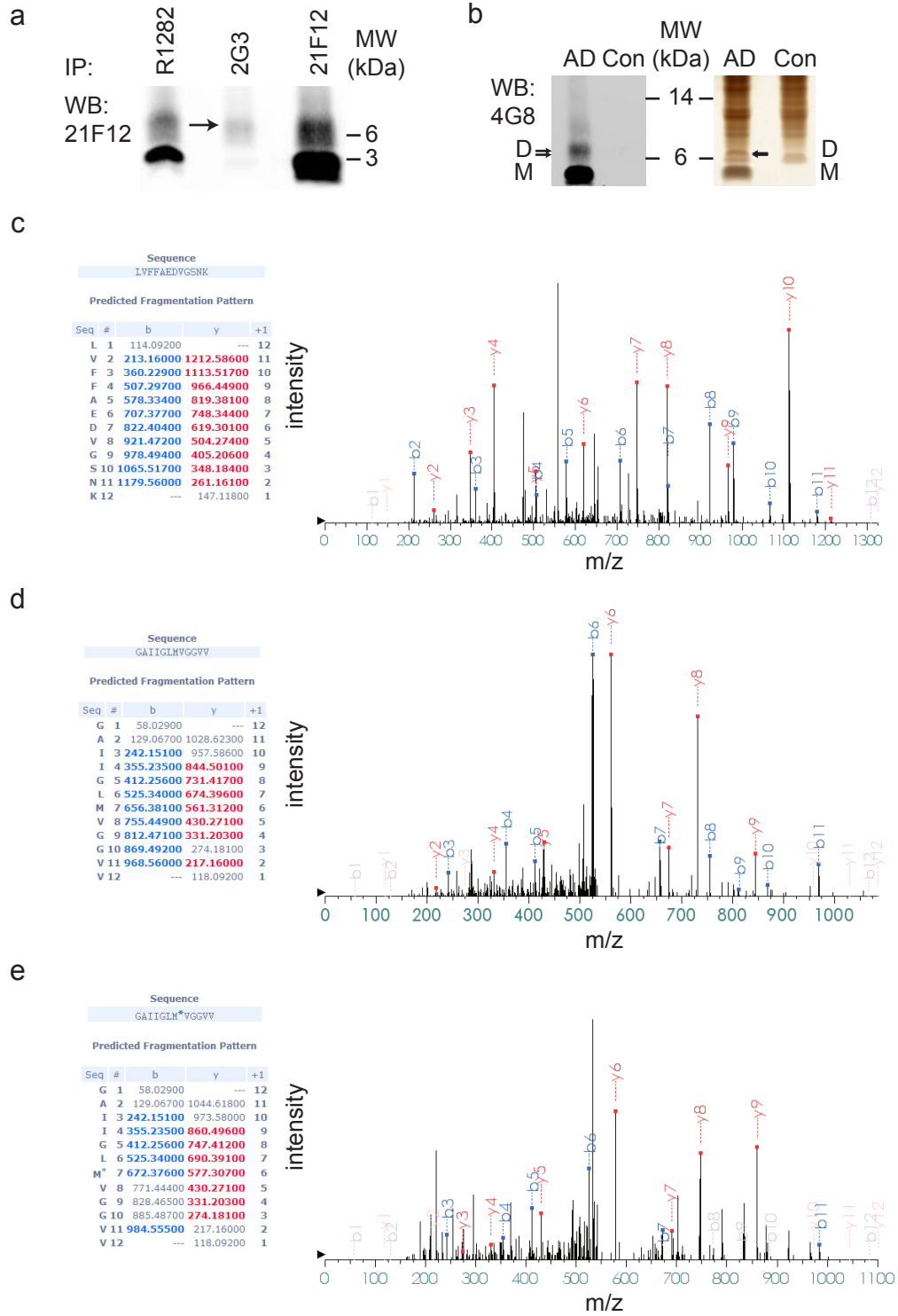
**Supplemental Figure 4.** Soluble A $\beta$  from AD brain decreases dendritic spine density through a NMDAR-dependent pathway. **a.** Representative images of apical dendrites from 5 DIV pyramidal cells in organotypic hippocampal slices cultured for an additional 10 days in sham condition or with SEC-enriched TBS extract from AD brain (AD TBS-SEC) or from Con brain (Con TBS-SEC). Scale bar = 5  $\mu$ m. **b.** Summary data for spine length. **c.** Representative images of slices treated with 500  $\mu$ M MCPG or 20  $\mu$ M CPP in the absence (sham) or presence of AD TBS-SEC.

Supplemental Figure 4



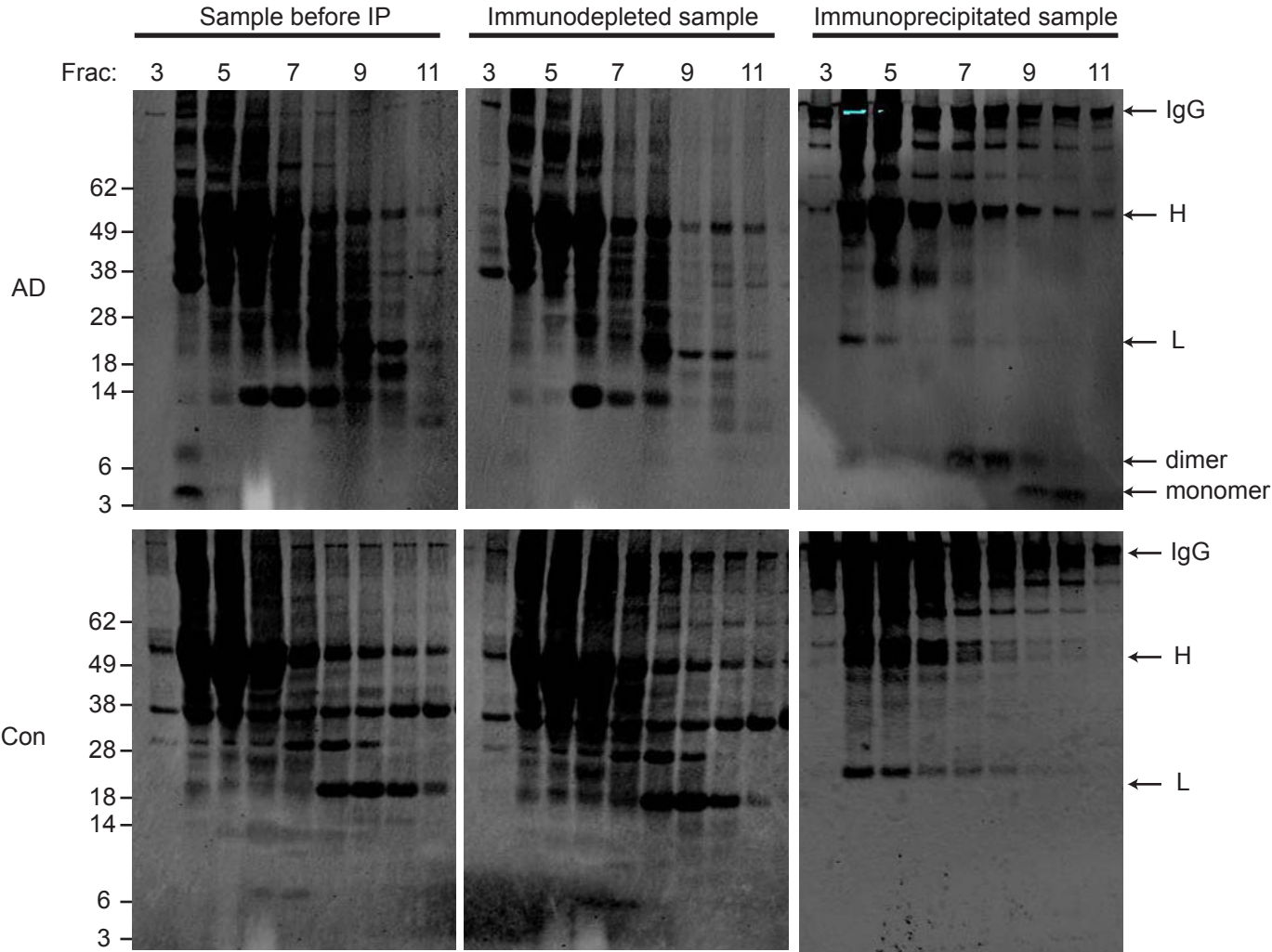
**Supplemental Figure 5.** Mass spectrometric confirmation of human A $\beta$  in the 8 kDa dimer band after IP of the GuHCl extract of an AD brain. **a.** A $\beta$  peptides ending in residue 40 (A $\beta$ <sub>40</sub>) or 42 (A $\beta$ <sub>42</sub>) can be detected uniquely by monoclonal antibodies 2G3 or 21F12, respectively. Insoluble (GuHCl) extract of AD brain was IP'ed with either 2G3 or 21F12 (or R1282 as a control), and all 3 precipitates were probed with 21F12. 21F12 detects an A $\beta$ <sub>40/42</sub> heterodimer (arrow) in the 2G3 IP but detects far more A $\beta$  dimers in the 21F12 IP, representing A $\beta$ <sub>42/42</sub> homodimers. **b.** GuHCl extracts of AD or control brain were IP'ed with a combination of 266, 2G3 and 21F12. WB with 4G8 (left panel) and silver staining (right panel) reveal bands in AD but not Con brain that correspond to the sizes of A $\beta$  monomer (M) and dimer (D). Bands identified as A $\beta$  monomer and dimer by WB and silver stain were digested with trypsin and the resulting peptides analyzed by LC-MS/MS. Analysis of the dimer band provided the sequences of: **c.** residues 17–28; **d.** residues 29–40; and **e.** residues 29–40 with an oxidized methionine at position 35 (a modification previously described in A $\beta$  from AD cortex<sup>1</sup>). The predicted peptide fragments are displayed vertically on the left and the observed mass-to-charge ratios are displayed horizontally on the right. Analysis of the monomer band provided the same peptide sequences (not shown). We did not recover the N-terminal tryptic fragment of A $\beta$  (residues 1–16) from either the 4 or 8 kDa bands, but IP with Asp-1 specific N-terminal A $\beta$  antibodies confirmed that these bands both contain A $\beta$  beginning at Asp-1 (e.g., see Supp. Fig. 2a).

Supplemental Figure 5



**Supplemental Figure 6.** A $\beta$  in AD TBS extracts can be purified and resolved as oligomer- and monomer-rich fractions by IP followed by SEC. AD TBS (top) or Con TBS (bottom) was IP'ed with 3D6 (3  $\mu$ g/mL), eluted with sample buffer containing 4% LDS and subjected to SEC. SEC of AD TBS without IP (top left) reveals that A $\beta$  monomers and dimers elute in fraction 4, which corresponds to the column void volume. This is detected by A $\beta$  C-terminal antibodies 2G3/21F12. Immunodepleted AD TBS (following IP with 3D6) reveals a similar pattern of background bands detected by WB (top center). SEC of the IP (top right) resolves A $\beta$  dimers (fractions 7/8) from monomers (fractions 9/10), as detected by 2G3/21F12 and 4G8. Fractions from the IP-SEC sample also contain intact immunoglobulin (IgG), and heavy chain (H) and light chain (L) fragments contributed by the immunoprecipitating antibody, as detected under these non-reducing conditions. As seen here and also by silver stain (not shown), the A $\beta$ -containing fractions following IP-SEC (top right) contain less background protein compared to the starting AD TBS extract (top left). Comparison of AD TBS and Con TBS blots reveals that the only novel species are the 4 and 8 kDa bands that exist only in AD TBS (not Con TBS, lower panels) and represent A $\beta$  monomer and dimer, respectively.

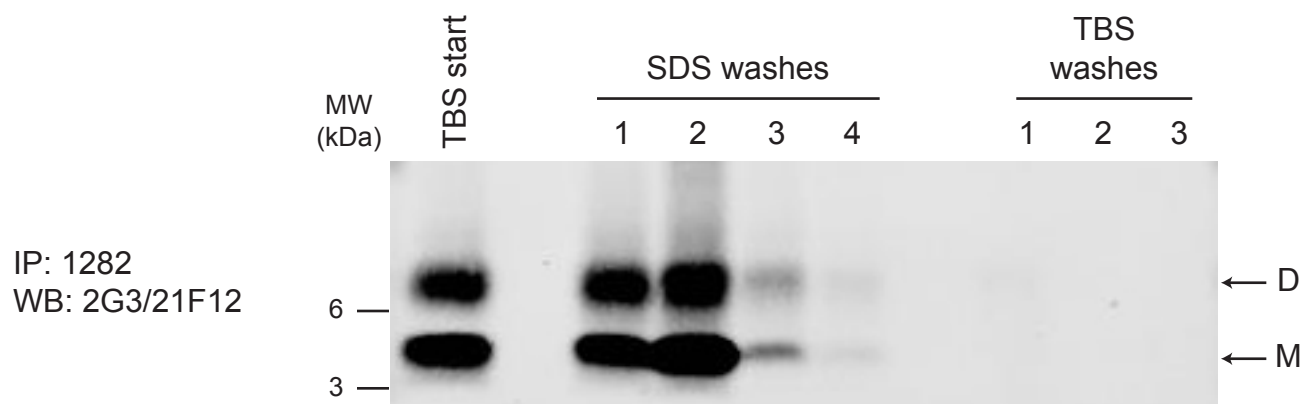
Supplemental Figure 6



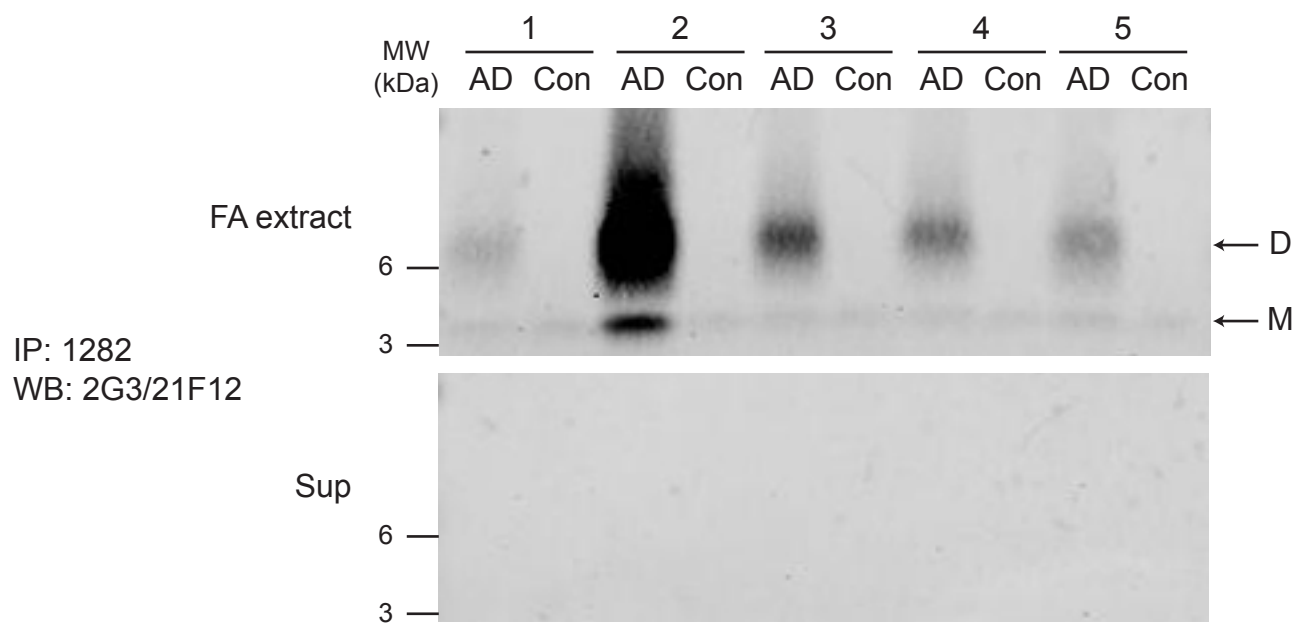
**Supplemental Figure 7.** Amyloid cores enriched from human AD cortex consist of dimers that are not readily released under physiologic conditions. **a.** Amyloid cores were prepared from AD brain tissue (100 mg wet wt) through sequential extractions with TBS and 2% SDS (as described in Methods and Figs. 6a, b). IP/WB analyses of wash supernatants reveal no additional soluble A $\beta$  species are liberated from the core prep by three final TBS washes after 4 sequential SDS washes. **b.** Amyloid cores remaining after the 7 sequential washes in (a) were subjected to a variety of incubation conditions to attempt the release of soluble A $\beta$  species. Sample 1 was cores prepared from 100 mg brain wet wt as in (a) and probed without further incubation. Samples 2–5 were cores prepared from 100 mg (samples 3–5) or 500 mg (sample 2) and then all incubated at 37°C for 24 hr. Samples 2 and 3 were incubated in 1% BSA in TBS (BSA was used to prevent non-specific loss of A $\beta$  on the wall of the siliconized tube during incubation). Sample 4 was sonicated for 1 min to increase amyloid core surface area then incubated in 1% BSA in TBS. Sample 5 was incubated in Con TBS to determine whether any soluble proteins in human brain extract could liberate A $\beta$  from the cores. IP/WB analysis of the post-500 g supernatants (bottom panel) and formic acid (FA) extracted pellets (top panel) reveal A $\beta$  dimers in the FA extracts of the remaining core pellet, but no soluble A $\beta$  released into the supernatant by these various treatments.

Supplemental Figure 7

a



b



**Supplemental Table 1. a.** Clinical and histopathological information on brain samples used for analysis in Fig. 1a. **b.** Clinical and histopathological information on brain samples used for analysis in Fig. 2a. Total A $\beta$  levels measured by ELISA in a subset of cases were 1.93 to 2.34 nmol A $\beta$ /g brain tissue in the insoluble extracts and 0.04 to 1.44 pmol A $\beta$ /g brain tissue in the soluble extracts of AD cortex, in range with previous reports<sup>2,3</sup>.

**a**

Case ID	Age	Clinical presentation	Neuropathological diagnosis
DS	60	Down syndrome, AD	AD
DLB	74	Possible CJD	Dementia with Lewy bodies
PCD	64	Recent onset of confusion and agitation	Paraneoplastic cerebellar degeneration
AD 1	73	Dementia	AD
MID 1	75	Recent onset of confusion	Stroke
AD 2	68	Dementia	AD
P-AD	78	Normal pressure hydrocephalus	AD
FTD	50	Frontotemporal dementia	Frontotemporal dementia
MID 2	69	Dementia	Multi-infarct dementia
AD 3	85	Dementia	AD

**b**

Case ID	Age	Clinical presentation	Neuropathological diagnosis
Con 1	75	Neurologically normal	Colloid cyst of third ventricle
Con 2	70	atypical dementia, possible AD or FTD	FTD
Con 3	52	Neurologically normal	Ventriculomegaly
AD 4	81	AD	AD
AD 5	80	AD	AD
AD 6	78	AD	AD
AD 7	82	AD	AD

## SUPPLEMENTAL METHODS

**Hippocampal slice preparation for electrophysiology recording.** Mice (C57BL/6 x 129, 5-8 wk old) were sacrificed after anesthesia with Isofen. The brain was quickly removed and submerged in ice-cold, oxygenated, sucrose-replaced artificial cerebrospinal fluid (ACSF) cutting solution (all in mM): 206 sucrose, 2 KCl, 2 MgSO<sub>4</sub>, 1.25 NaH<sub>2</sub>PO<sub>4</sub>, 1 CaCl<sub>2</sub>, 1 MgCl<sub>2</sub>, 26 NaHCO<sub>3</sub>, 10 D-glucose, pH 7.4, 315 mOsm. Transverse slices (350 μm thickness) from the middle portion of each hippocampus were cut with a Vibroslicer. After dissection, slices were incubated in ACSF that contained (all in mM): 124 NaCl, 2 KCl, 2 MgSO<sub>4</sub>, 1.25 NaH<sub>2</sub>PO<sub>4</sub>, 2 CaCl<sub>2</sub>, 26 NaHCO<sub>3</sub>, 10 D-glucose, pH 7.4, 310 mOsm, in which buffer they were allowed to recover for at least 90 min before recording. A single slice was then transferred to the recording chamber and submerged beneath a continuous ACSF perfusate saturated with 95% O<sub>2</sub> and 5% CO<sub>2</sub>. Slices were incubated in the recording chamber for 20 min before stimulation at RT (~26°C).

**Dendritic spine density analysis.** The apical dendrites of pyramidal cells in organotypic hippocampal slices were prepared, treated, imaged and analyzed as described<sup>4</sup>. Briefly, 2 days after organotypic hippocampal slices were prepared from postnatal day 5 (P5) - P7 Sprague-Dawley rats, the slices were biolistically transfected with eGFP-N1 (Clontech, Cambridge, UK). After an additional 3 d of culturing, the various reported treatments were performed for an additional 10 d. All Aβ containing SEC fractions from AD TBS (AD TBS-SEC) and the corresponding fractions from Con TBS (Con TBS-SEC) were pooled separately and lyophilized prior to addition to the culture medium of organotypic hippocampal slice preparations. For treatment with Con TBS-SEC or AD TBS-SEC 350 μL lyophilized SEC fractions of the human brain TBS extract were reconstituted in 3 mL slice culture medium (SCM). 750 μL of this prep were applied to each insert in a 6-well plate. Either D-CPP (20 μM) or (R/S)-MCPG (500 μM) were added to sham or AD TBS-gf treated slices. For treatment with the GuHCl extract SEC fractions, a 450 μL lyophilized fraction was reconstituted in 4.5 mL SCM, of which 750 μL were added to each insert. The media were changed with fresh medium containing these treatments every 2-3 d. At the end of the 10-day treatment, live-cell imaging was performed on the inserts after submerging in ACSF. Apical dendrites were imaged by 2-photon laser scanning microscopy using a 5x zoom corresponding to 42 μm x 42 μm. Analysis on the acquired images was performed blinded to treatment using custom software designed in Matlab. Statistical analyses were performed using Igor Pro (Wavemetrics, Lake Oswego, OR).

**Passive Avoidance Conditioning.** Passive avoidance training was performed as described previously<sup>5</sup> (see Supplemental Methods). Wistar rats were obtained from the Biomedical Facility at University College Dublin, and all procedures were conducted in accordance with animal welfare guidelines of the Department of Health and Children (Republic of Ireland). Animals were cannulated at P70 and handled for 6 days prior to training at P80. Weight was measured and behavior was assessed in an open-field apparatus for 5 min periods at 48 and 24 h before training. Locomotion, rearing, grooming, piloerection, defecation and posture were studied to assess post-surgical alterations in behavior. Animals were trained in a single-trial, step-through, light-dark passive avoidance paradigm. The training apparatus chamber was divided into two

compartments, separated by a central shutter that contained a small opening. The smaller of the compartments contained a low-power illumination source; the larger compartment was not illuminated. The floor in the dark compartment consisted of a grid of 16 horizontal stainless-steel bars. A current generator supplied 0.75 mA to the floor, which was scrambled once every 0.5s across the 16 bars. A resistance range of 40–60 mΩ was calculated for a control group of rats (250–350 g), and the apparatus was calibrated accordingly. On the day of training, animals were placed facing the rear of the light compartment of the apparatus, immediately after spontaneous behavior was assessed. The timer was started once the animal completely turned to face the front of the chamber. Latency to enter the dark chamber was recorded (usually <20 s). After the animal completely entered the dark compartment a foot shock was administered to the animal, at which point the subject immediately returned to the light compartment. Animals were then returned to their home cages. At 0, 3, or 6h following this training session, 5 μL soluble human cortical extract was introduced i.c.v. through the cannula at 1μL/min. Recall of the passive avoidance conditioning was evaluated 24 and 48 h post-training by recording the latency to enter the dark chamber, with a criterion time of 300s. Data from the passive avoidance studies were analyzed by ANOVA followed by the Bonferroni post hoc test.

**IP-SEC.** TBS extracts of AD or control cortex were immunoprecipitated with 3D6 (3 μg/mL), 15 μL PAS and 15 μL PGA. After the beads were washed, the immunoprecipitates were eluted with 10 μL 4% LDS sample buffer, heated at 65°C for 5 min and centrifuged at 14,000 rpm for 5 min. The supernate was transferred to 500 μL TBS and subjected to SEC as described above.

**Quantification of Aβ in brain extract.** Aβ levels in the brain extract were analyzed by sandwich enzyme-linked immunosorbent assay (ELISA) as described previously<sup>6</sup>. Briefly, 2G3 and 21F12 was used to capture Aβ<sub>40</sub> and Aβ<sub>42</sub>, respectively. Following capture, biotinylated 3D6 or biotinylated 4G8 was used to quantify TBS or GuHCl extracted Aβ, respectively.

**Mass spec methods.** Mass spectrometry experiments were performed at the Taplin Biological Mass Spectrometry Facility at Harvard Medical School. Gel bands containing Aβ samples were digested with trypsin and then analyzed by nanoscale microcapillary liquid chromatography coupled to tandem mass spectrometry as described<sup>7</sup>.

**Production & characterization of cross-linked synthetic dimers.** Aβ<sub>1-40</sub>S26C was synthesized by the Biopolymer Laboratory at UCLA Medical School and the correct sequence and purity confirmed by amino acid analysis, reverse-phase HPLC and mass spectrometry. Aβ dimers were generated by atmospheric oxidation of a 20 μM solution of Aβ<sub>1-40</sub>S26C in 20 mM ammonium bicarbonate, pH 8.0, for 4 days at room temperature. To facilitate disassembly of aggregates formed during the oxidation reaction, the peptide solution was lyophilized and subsequently incubated in 5 M GuHCl, Tris-HCl, pH 8.0, for 4 hr. Disulfide cross-linked Aβ dimers were isolated from unreacted monomer and higher aggregates by size exclusion chromatography. Briefly, two Superdex 75 10/30 HR columns were linked in series and eluted with 50 mM

ammonium acetate, pH 8.5 at a flow rate of 0.5 ml/min. Fractions (0.5 ml) were collected, and an aliquot of each was electrophoresed on 16% tris-tricine polyacrylamide gels and detected by silver staining. Fractions found to contain exclusively dimeric A $\beta$  were pooled and the peptide content determined by comparison to known standards. Samples were stored at -80°C until used.

**Isolation of amyloid cores.** The pellet resulting from spinning the TBS homogenate at 175,000 g for 30 min (TBS start) was resuspended in 150  $\mu$ L 2% SDS per 100 mg starting brain wet weight, boiled at 100°C for 5 min, and centrifuged at 10,000g for 5 min. The supernatant was collected (SDS Wash 1) and the pellet was extracted similarly with SDS an additional 3 times (SDS Washes 2-4). The remaining pellet was resuspended in 150  $\mu$ L TBS per 100 mg starting brain wet weight and centrifuged at 500 g for 5 min. The supernatant was collected (TBS Wash 1) and the pellet was washed with TBS an additional two times (TBS Wash 2-3). The resulting washed core prep (following a final centrifugation at 500 g for 5 min) was incubated with 10  $\mu$ L 88% formic acid per 100 mg starting brain weight at RT for 2 hr. This sample was neutralized with 2.6 vol 10 N NaOH prior to IP/WB analysis or treatment of acute hippocampal slices. Intact cores (following the final TBS wash) were centrifuged at 500 g and resuspended in 0.2% Congo red for visualization by brightfield and polarized microscopy.

## REFERENCES

1. Naslund, J. et al. Relative abundance of Alzheimer A beta amyloid peptide variants in Alzheimer disease and normal aging. *Proc Natl Acad Sci U S A* **91**, 8378-82 (1994).
2. Lue, L.F. et al. Soluble amyloid beta peptide concentration as a predictor of synaptic change in Alzheimer's disease. *Am J Pathol* **155**, 853-62 (1999).
3. Naslund, J. et al. Correlation between elevated levels of amyloid beta-peptide in the brain and cognitive decline. *Jama* **283**, 1571-7 (2000).
4. Shankar, G.M. et al. Natural oligomers of the Alzheimer amyloid-beta protein induce reversible synapse loss by modulating an NMDA-type glutamate receptor-dependent signaling pathway. *J Neurosci* **27**, 2866-75 (2007).
5. Fox, G.B., O'Connell, A.W., Murphy, K.J. & Regan, C.M. Memory consolidation induces a transient and time-dependent increase in the frequency of neural cell adhesion molecule polysialylated cells in the adult rat hippocampus. *J Neurochem* **65**, 2796-9 (1995).
6. Sun, X. et al. Lithium inhibits amyloid secretion in COS7 cells transfected with amyloid precursor protein C100. *Neurosci Lett* **321**, 61-4 (2002).
7. Haas, W. et al. Optimization and use of peptide mass measurement accuracy in shotgun proteomics. *Mol Cell Proteomics* **5**, 1326-37 (2006).